

**Republic of Iraq**  
**Ministry of Higher Education**  
**and Scientific Research**  
**University of Diyala**  
**College of Science**  
**Department of Physics**



# **Fabrication and characterization of PES/PVP blend membranes incorporated with Ag based materials for water purification applications**

**A Thesis Submitted to the Council of the College of Science-  
University of Diyala in Partial Fulfillment of the Requirements for  
the Degree of Doctor of Philosophy of Science in Physics**

**By**

**Sabah Ali Khadhir**

**Supervised By**

**Assist. Prof. Dr. Ammar Ayesh Habeeb**

**Assist. Prof. Dr. Muhannad Mahdi Abd**

**2026 A.D.**

**1447 A.H.**

## Abstract

In this thesis, polymeric membranes embedded with silver-based materials were fabricated to enhance pollutant removal from water, while exhibiting porous, flexible, antibacterial, and photocatalytic properties. The work was carried out in two main stages. In the first stage, silver nanoparticles were prepared using the chemical method and pulsed laser ablation in liquids. The second stage involved incorporating these nanoparticles into a polymeric matrix composed of polyether sulfone (PES) as the main material, with polyvinylpyrrolidone (PVP) and calcium carbonate ( $\text{CaCO}_3$ ) added as pore-forming and permeability-enhancing agents.

The structural properties of the prepared nanoparticles were analyzed using (XRD) X-ray diffraction. The patterns of the chemically prepared samples in order A1-  $\text{AgO}_1$  (reference), A2 ( $\text{AgO-AgCl}$ ), A3 ( $\text{AgO-AgCl}$ ), and A4 ( $\text{AgO}$ ) showed distinct diffraction peaks at (111), (200), (220), and (311) planes, confirming the formation of crystalline ( $\text{AgO}$ ) with a face-centered cubic (FCC) structure. Additional peaks were observed in some samples, particularly A2 and A3, corresponding to the presence of silver chloride ( $\text{AgCl}$ ), indicating the formation of mixed phases due to the preparation conditions. Calculations showed that the average crystallite size of the chemically prepared samples was approximately 33 nm. In contrast, the use of pulsed laser ablation in liquids for samples A5 ( $\text{Ag-AgO}$ ), A6 ( $\text{Ag-AgO}$ ), A7 ( $\text{Ag-AgO}$ ), and A8 ( $\text{Ag-AgO}$ ) resulted in smaller and more uniform nanoparticles, with an average crystallite size of about 25 nm, reflecting the impact of the preparation method on crystal size and uniformity.

(FTIR) Fourier transform infrared confirmed the presence of  $\text{Ag-O}$  bonds in the  $400\text{--}600\text{ cm}^{-1}$  range, indicating successful formation of silver oxide. A broad band observed at  $3400\text{ cm}^{-1}$  was attributed to hydroxyl group vibrations associated with moisture adsorbed on the nanoparticle surfaces. Other bands related to surface functional groups were also observed, indicating good chemical stability of the prepared materials.

(UV-Vis) UV-vis absorption spectra showed that the chemical samples (A1-A4) exhibited absorption peaks at wavelengths below 300 nm, indicating the formation of  $\text{AgO}$  and  $\text{AgCl}$ .

The laser samples (A5-A8) for UV-Vis showed surface plasmon resonance peaks at 410-427 nm, confirming the presence of stable silver molecules.

(SEM) Scanning Electron Microscopy images revealed clear differences in shape and size depending on the preparation method. Sample A1 consisted of nanoparticles with a size distribution between 24 and 51 nm and slight aggregation, while the other chemically prepared samples (A2–A4) exhibited larger and more heterogeneous particles ranging from 205 to 323 nm. The laser-prepared samples (A5–A8) showed more uniform distributions of spherical and cubic particles, with sizes ranging from 57 to 107 nm, demonstrating the ability of laser techniques to produce highly uniform nanoparticles.

(EDS) Energy Dispersive X-ray confirmed the presence of silver and oxygen as the main components in all samples, supporting the XRD and FTIR results regarding silver oxide formation. The silver content was higher than oxygen, indicating good purity of the materials. Additionally, (ZP) zeta potential measurements indicated high stability in the liquid medium, with values ranging from 35.71 to -45.91 mV, reflecting sufficient electrostatic repulsion to prevent aggregation and maintain uniformity, with particle sizes varying according to the preparation method.

In the application aspect, the nanoparticles exhibited significant biological activity. The antibacterial effect increased with higher concentrations against two bacterial strains, showing clear inhibition at higher concentrations.

Cytotoxicity tests for samples A1, A4, A5, and A8 showed moderate toxicity, with A4 recording the highest toxicity value of 15.6.

Photocatalytic, the samples demonstrated good photocatalytic efficiency in degrading contaminated blue dye under visible light, with removal efficiencies of 70% for A1 and 79% for A3 after 150 minutes of irradiation.

Regarding the PES/PVP polymeric membranes embedded with silver nanoparticles, ATR-FTIR analysis confirmed successful incorporation of the nanoparticles within the polymeric matrix. Embedding silver oxide into the membranes improved surface properties.

The contact angle decreased from 83° to 65° and 58° with increasing silver oxide content, indicating improved hygroscopicity. The water flow rate increased from 82 L/m<sup>2</sup>/h for the unmodified membranes to 115 and 132 L/m<sup>2</sup>/h, reflecting greater water permeability.

(SEM) analysis revealed that the prepared membranes possess a spongy porous structure with interconnected cavities and channels, enabling efficient water permeability. (FESEM) Field Emission Scanning Electron Microscopy side-view examination showed distinct variations in pore size and layer thickness depending on the fabrication method. Notably, the membranes reinforced with laser-engineered nanoparticles demonstrated superior antibacterial performance, achieving inhibition rates of 95–99%, highlighting their promising potential for water purification and contaminant removal. Biological evaluations confirmed a significant improvement in antibacterial activity, increasing from 13–41% in the original membranes to 72–73% with the addition of silver powder, and reaching 95–99% after incorporating laser-engineered silver oxide nanoparticles. Overall, these results demonstrate that silver oxide modification significantly enhances membrane functionality, making them suitable for water treatment applications.

# **Chapter One**

## **Introduction & Literature Review**

## 1.1. Introduction

This chapter introduces the main themes of the thesis and provides a review of relevant previous studies. It also highlights the major factors contributing to the growing global concern over the shortage of potable water, which has increased interest in advanced technologies and alternative methods for producing clean water. Among these approaches, polymer membranes have received significant attention due to their versatile properties and structural stability. In recent years, extensive research has been directed toward the development of high-flux membranes that offer flexibility, withstand operational pressures, and contribute to lowering overall operating costs [1]. Evaporation and condensation are among the earliest techniques used for water purification; however, they are associated with high operating costs, long processing times, and adverse environmental impacts. Over the past decades, research efforts have focused on advancing membrane technologies to improve their efficiency in producing potable water. This has resulted in the development of modern techniques, such as reverse osmosis membranes, which exhibit reduced environmental impact and lower chlorine content in treated water. Numerous studies have investigated membrane modification strategies, including structural optimization and surface modification through the incorporation of chemical and polymeric layers, to enhance water permeability and separation efficiency. These advancements have enabled the production of high-purity water through effective removal of salts and contaminants, while also improving resistance to the passage of microorganisms such as bacteria, fungi, and viruses. Furthermore, the incorporation of various nanoparticles into polymeric membranes has been employed to minimize agglomeration during fabrication, thereby enhancing overall membrane performance [2].

Due to population growth, extensive agricultural irrigation, and pollution from sewage and industrial wastewater, the world is facing a serious and increasing shortage of water resources, which has made access to clean drinking water increasingly challenging. Consequently, various technologies have been developed for desalinating saline water and treating stagnant or contaminated water, with membrane-based processes being among the most prominent. These include polymer membranes, reverse osmosis membranes, and structural modifications through the incorporation of polymeric layers to enhance porosity. In addition, the integration of nanomaterials, polymers, and other surface coatings has been widely adopted to improve water permeability and overall membrane performance [3].

## 1.2 .Silver Nanoparticles

Silver nanoparticles (AgNPs) are among the most extensively studied nanomaterials in environmental and biomedical applications, particularly in water treatment systems, due to their unique physicochemical properties at the nanoscale. Their high antimicrobial activity is mainly attributed to their high surface-to-volume ratio, which enhances interactions with microorganisms. Silver nanoparticles inhibit or destroy microbial cells by penetrating cell membranes and interacting with cellular proteins and DNA, thereby disrupting essential biological functions. In membrane-based applications, silver nanoparticles can be incorporated into the polymer matrix or immobilized on the membrane surface, improving antifouling properties and effectively inhibiting bacterial, fungal, and viral growth. Moreover, these nanoparticles exhibit advanced characteristics such as surface plasmon resonance (SPR), high surface reactivity, enhanced contaminant removal efficiency, and good biocompatibility, making them highly suitable for water purification applications [4]. Table

(1.1), shows Physical, Chemical, and Crystalline Properties of Silver Nanoparticles. Figure (1.1), shows the molecular structure of isolated Ag.

**Table (1.1): Physical, Chemical, and Crystalline Properties of Silver Nanoparticles [5].**

Property	Description / Value	Notes
Morphology	Spherical, quasi-spherical, sometimes rod-like	Depends on synthesis method
Particle Size (nm)	(10–50) nm varies depending on synthesis	Size affects antimicrobial activity
Surface-to-volume ratio	Very high	Responsible for antimicrobial activity
Antimicrobial activity	Very high	Inhibits bacteria, fungi, and viruses
Crystal structure	FCC (Face-Centered Cubic)	Confirmed by XRD
Optical properties	Surface plasmon resonance (SPR)	Typically observed at 400–450 nm
Surface reactivity	High	Enhances contaminant removal
Biocompatibility	Good	Suitable for environmental and biomedical applications

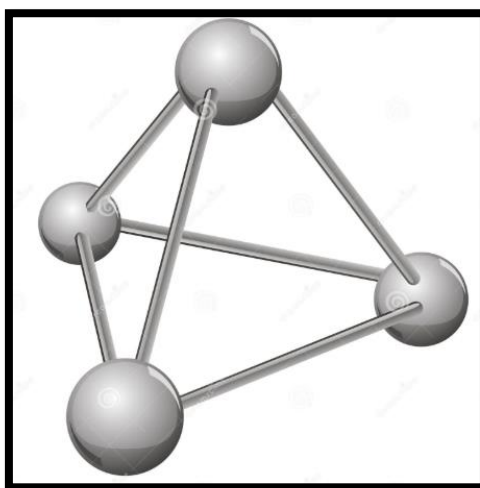


**Figure (1.1). The molecular structure of isolated Ag.**

### 1.3. Nano Silver Oxides

Silver oxide nanoparticles ( $\text{Ag}_2\text{O}$  NPs) are among the fastest-growing classes of nanomaterials in recent years due to their unique

physicochemical and biological properties. These nanoparticles exhibit a dual functionality, combining the strong antimicrobial activity of silver with the oxidative activity of silver oxides. This has attracted significant scientific interest and led to their extensive application in water-related technologies and biomedical fields. Numerous studies have shown that Ag<sub>2</sub>O NPs possess strong antimicrobial properties, act as effective drug carriers, and exhibit antiviral, antioxidant, and anti-inflammatory activities. These properties are largely attributed to their high surface area and enhanced surface reactivity at the nanoscale, which facilitate effective interactions with biological systems [6]. The biological mechanisms of action of nano silver oxides involve multiple pathways within microbial cells. These materials inhibit DNA replication and disrupt the integrity of the plasma membrane, resulting in increased membrane permeability and leakage of cytoplasmic contents. In addition, they interfere with nutrient transport into the cell, leading to metabolic dysfunction, necrosis, and ultimately cell death. Collectively, these mechanisms account for the high antimicrobial efficiency of nano silver oxides against a wide range of microorganisms [7]. Figure (1.2), shows Molecular structure of the Ag<sub>2</sub>O [8]. And table (1.2), shows Physical, Chemical, and Biological Properties of (Ag<sub>2</sub>O NPs) [9].

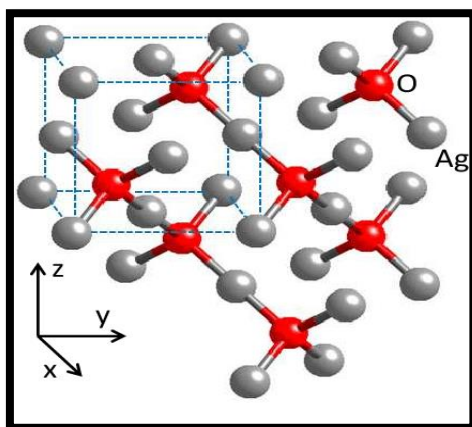


Figure (1.2). Molecular structure of the Ag<sub>2</sub>O [8].

**Table (1.2): Physical, Chemical, and Biological Properties of (Ag<sub>2</sub>O NPs) [9].**

Property	Description / Value	Notes
Morphology	Mostly spherical	Shape can vary depending on synthesis method
Particle Size (nm)	~10–45 nm (average ~25 nm)	Size depends on synthesis method
Surface-to-volume ratio	Cubic lattice	Confirmed by XRD
Antimicrobial activity	SPR peak at ~435 nm	Indicates nanoscale formation
Crystal structure	Strong antibacterial and antifungal activity	Effective even against resistant strains
Optical properties	High free radical scavenging potential	Linked to surface reactivity and phytochemical capping
Surface reactivity	High	Enhances interactions with biomolecules and reactive species
Biocompatibility	Moderate to good depending on synthesis	Green synthesis generally reduces toxicity

## 1.4. Silver Chloride

Silver chloride (AgCl) is an important nanomaterial that has received extensive scientific attention in photocatalytic and water treatment applications due to its unique physicochemical properties. AgCl features a wide energy band gap of approximately 5.2 eV, enabling the activation of photocatalytic reactions under specific light wavelengths. This property allows for the efficient degradation of contaminant dyes and stable organic pollutants in water, thereby enhancing water purification processes [10]. Table (1.3), shows Physical and Chemical Properties AgCl NPs[11] . Figure (1.3), shows Molecular structure of the AgCl.

Table (1.3): Physical and Chemical Properties (AgCl NPs) [11].

Property	Description / Value	Notes
Morphology	Spherical or quasi-spherical, sometimes cubic	Depends on synthesis method
Particle Size (nm)	15–60 nm	Average size depends on synthesis
Surface-to-volume ratio	FCC / Cubic lattice	Confirmed by XRD
Antimicrobial activity	~5.2 eV	Determines photocatalytic activity
Crystal structure	UV absorption / Max absorption ~380–400 nm	Indicates photocatalytic potential
Optical properties	High	Efficient for degradation of dyes and organic pollutants
Surface reactivity	High	Enhances adsorption and interaction with pollutants

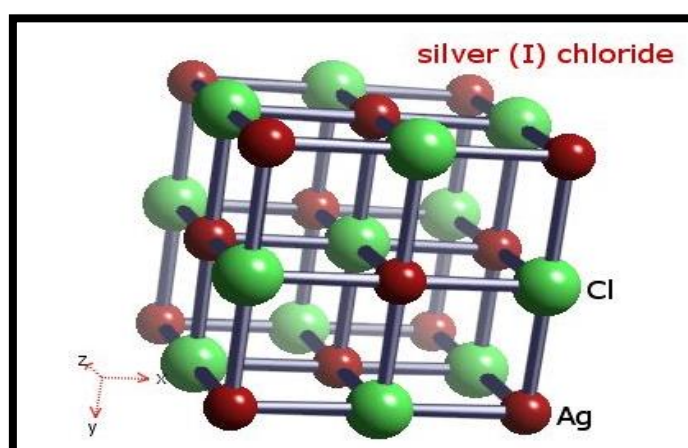
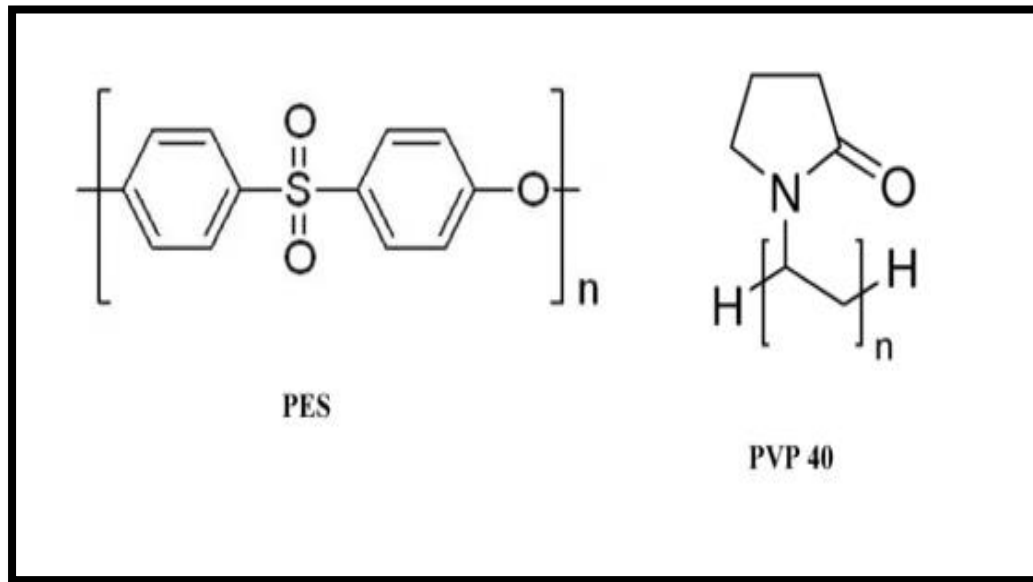


Figure (1.3). Molecular structure of the AgCl.

## 1.5. Polymer Membranes (PES/PVP)

Polyether Sulfone (PES) is one of the most widely used polymers in membrane fabrication due to its high thermal, chemical, and mechanical stability, which allows membranes to maintain their structural integrity and functional performance under diverse operating conditions, including high temperatures, elevated pressures, and exposure to harsh chemicals. PES

also exhibits strong mechanical strength and hydraulic resistance, making it suitable for membranes applied in water desalination, industrial water treatment, and wastewater purification. Figure (1.4), shows Molecular structure of the PES-PVP polymer [12].



**Figure (1.4). Molecular structure of the PES-PVP polymer [12].**

To enhance water permeability and pore formation, hydrophilic additives such as Polyvinylpyrrolidone (PVP) are incorporated. PVP increases membrane hydration and reduces hydrophobicity, facilitating water transport and improving water flux. It also contributes to the formation of uniform and well-distributed pores during membrane fabrication, enhancing contaminant and particle separation. Membranes modified with PVP show improved resistance to biofouling, as the increased porosity and hydrophilic surface help prevent bacterial and fungal adhesion, prolonging membrane lifespan and maintaining performance over time [13]. Incorporation of inorganic materials such as calcium carbonate (CaCO<sub>3</sub>) enhances mechanical strength and surface characteristics by forming uniform pores, which increase water flux and improve separation efficiency. Furthermore, combining polymers with nanomaterials to create

hybrid membranes effectively improves antifouling performance, offering high water permeability, enhanced pollutant rejection, and tailored properties for water purification, wastewater treatment, and desalination applications [14]. Table (1.4), shows Properties of PES/PVP and Hybrid Membranes. And figure (1.5), shows molecular structure of the  $\text{CaCO}_3$ .

**Table (1.4): Properties of PES/PVP and Hybrid Membranes [13].**

Feature	Description / Value	Notes
Polymer Type	Polyether Sulfone (PES)	High thermal, chemical, mechanical stability
Hydrophilic Additive	Polyvinylpyrrolidone (PVP)	Improves hydration, reduces hydrophobicity, facilitates pore formation
Pore Structure	Uniform, well-distributed	Enhances water flux and contaminant separation
Mechanical Strength	High	Maintains integrity under high pressure and chemical exposure
Hydraulic Resistance	Strong	Suitable for industrial water treatment
Biofouling Resistance	Improved with PVP	Hydrophilic surface and porosity reduce bacterial/fungal adhesion
Inorganic Additives	Calcium carbonate ( $\text{CaCO}_3$ )	Enhances mechanical strength and water flux
Hybrid Nanocomposites	PES/Nanomaterial membranes	High water permeability, pollutant rejection, antifouling
Applications	Desalination, industrial water treatment, wastewater purification	Long-term stability and high performance

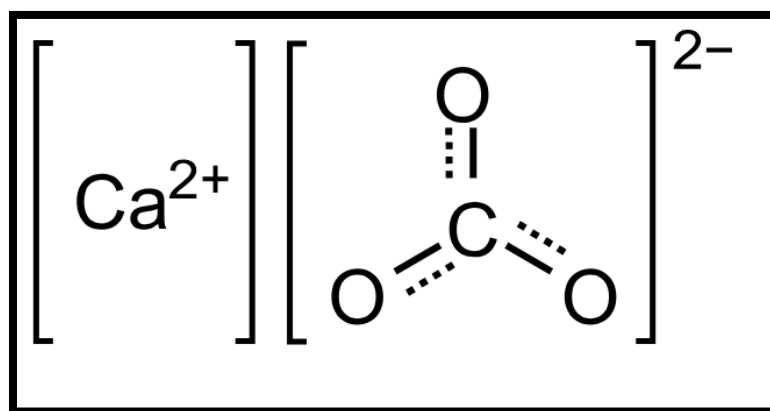


**Figure (1.5). Molecular structure of the  $\text{CaCO}_3$  [15].**

## 1.6. Literature Review

**In 2015, Al-Habib et al.**, prepared polyamide polymer membranes reinforced with silver oxide ( $\text{Ag}_2\text{O}$ ) nanoparticles ranging in size from 20 to 50 nm. A thin polyamide film was produced using interlayer polymerization combined with reverse osmosis and then deposited onto a Polysulfone substrate reinforced with the nanoparticles. Various analyses of the membranes, along with contact angle measurements, showed that the silver oxide distribution within the polyamide layer was uniform, resulting in an increase in water flow rate from 26 to 40.5 L/m<sup>2</sup>/hr, while maintaining a salt rejection rate of less than 2%, performance similar to that of the original polyamide membrane [16].

**In 2016, Nasab et al.**, reported the fabrication of hybrid membranes incorporating silver oxide ( $\text{AgO}$ ) nanoparticles via precipitation using silver nitrate as a starting material in an aqueous solution. The structural, morphological, and optical properties of the silver oxide nanoparticles were demonstrated using FTIR, XRD, SEM, EDS, and catalytic activity techniques. The results showed that the silver oxide nanoparticles achieved catalysis and photodegradation of the dye after 60 minutes of exposure to visible light indicating their high capacity for removing rhodamine-B dye [17].

**In 2017, Gul et al.**, fabricated nanofilms composed of Polyether Sulfone (PES) and Cellulose Acetate (CA) incorporating silver oxide ( $\text{Ag}_2\text{O}$ ) using casting and bonding method. Structural, morphological, and compositional analyses confirmed the presence of a silver phase within the membrane, a homogeneous distribution of the cast layer in the polymer matrix, and the formation of strong bonds between its components. Experimental results demonstrated that the fabricated membrane exhibited an enhanced water

permeability rate of 92.88 L/h/m<sup>2</sup>/bar and a reduced contact angle of 63.5°, indicating increased hydrophilicity. The Bovine Serum Albumin (BSA) rejection also increased to 88.8%, reflecting improved separation efficiency. Moreover, the hybrid membrane displayed antimicrobial activity, enhancing the performance of water purification membranes and confirming its potential for environmental and health-related applications [18].

**In 2017, Shen et al.**, prepared silver oxide (AgO) from silver nitrate and applied it to bacteria to investigate its biological effects. The phase structure changes of silver oxide nanoparticles upon bacterial exposure and the cellular responses were analyzed using X-ray diffraction (XRD). The results demonstrated effective bacterial inhibition and Ag<sub>3</sub>PO<sub>4</sub>-induced cell death. The antibacterial activity of silver oxide nanoparticles occurred through multiple mechanisms, primarily through the release of silver ions, which caused cytotoxicity and damage to the bacterial cell membrane [19].

**In 2018, Wai, K. P, et al.**, deposited silver nanoparticles onto Polyether Sulfone (PES) membranes that had been functionalized with Polydopamine via a redox process. Polyvinylpyrrolidone (PVP) was incorporated to increase porosity and water permeability. Four multilayer membranes were fabricated for performance evaluation, PES pure membrane1, membrane2 with PES -PVP, membrane 3 Polydopamine with PES and PVP, membrane4 with Ag Polydopamine and PES- PVP. The membranes were evaluated for pure water flux, antimicrobial activity, and humic acid rejection. The results showed that membrane1 achieved a water flux of 27.16 L/m<sup>2</sup>/h/bar with 84% humic acid removal. Adding PVP in membrane2 increased water flux but slightly reduced humic acid rejection. In contrast, membrane4, with Polydopamine and silver, showed improved

water permeability, enhanced antimicrobial activity, and the highest humic acid rejection [20].

**In 2019, Shahat et al.**, reported a wet chemical method that provides a rapid, simple, and cost-effective approach for the synthesis of silver oxide nanoparticles using aspirin as a precursor. The resulting material was tested against microorganisms, including bacterial strains such as *Escherichia coli* and fungal strains, using the agar plate diffusion method. The nanoparticles were further characterized using FTIR, SEM, TEM, and XRD techniques. The results demonstrated high antimicrobial activity, effectively inhibiting the growth of both bacteria and fungi, confirming their potential as antimicrobial agents. Moreover, the nanoparticles incorporated with Asp/SONPs/PVA exhibited anthelmintic activity, inducing either paralysis or death in worms. Additionally, the data indicated that silver nanoparticles possess cytotoxic effects, suggesting potential applications as pesticides, while also highlighting their possible phytotoxicity [21].

**in 2020 Yang et al.**, made three types of graphene oxide (GO/AgNP) composite sheets to look at how silver nanoparticles interact with nanofiltration at sizes of 8, 20, and 33 nm. After that, X-ray diffraction (XRD) was used to test the films to see how well the silver had been added and how well they worked in terms of their optical properties, huge energy gap, and good surface and particle distribution. The composite film had the highest water flux (106.1 L/m<sup>2</sup>h/bar), the highest dye rejection rate (RhB), and the highest efficiency (97.73%) compared to the other films. This was done to test the filtering performance in a closed 20 nm filter. The distance between the layers and the size of the defects had a big effect on the nanofiltration process. This suggests that there are two independent mechanisms that determine how well the film works [22].

**In 2021, Li et al.,** produced regular spherical silver oxide nanoparticles (Ag<sub>2</sub>O NPs) measuring 30 nm and the results indicated a full 100 percent inhibition rate demonstrating their potent antimicrobial properties. It also revealed that it caused damage to the cell membrane and oxidative stress on the cell caused by silver oxide nanoparticles, and confirms its potential for use as bactericidal agents as well [23].

**In 2022, Alamer et al.,** developed a green biosynthetic approach for producing silver chloride nanoparticles (AgCl-NPs) using *Bacillus mojavensis* from rhizospheric soil. Analyses using (XRD) (FTIR) (SEM) and (TEM) techniques proved the presence of spherical nanoparticles (5-35 nm) with a face-centered cubic (FCC) structure of silver-silver chloride (Ag/AgCl) and that (AgCl-NPs) have strong antibacterial activity against *Ralstonia solanacearum* at a concentration of 20 µg/ml indicating the possibility of their use as environmentally friendly nano-biopesticides [24].

**In 2022, Wu et al.,** fabricated thin-layer water treatment membranes (TFC-FO) on a Polysulfone substrate. The change was intended to lower internal concentration polarization (ICP) while preventing the membrane from turning dirty. The membranes that had (BiOAg) nanoparticles in them were more porous and had a lower ICP. Water might flow through them 2.5 to 4.4 times faster than the original TFC-FO membranes. After being in water for 30 days the membranes themselves likewise improved better and maintained 96.5% of the removed silver that was taken out. The results show that changing the substrate is a good way to improve ICP performance and resistance to infection [25].

**In 2023, Al-Mousoi et al.,** worked on producing silver oxide nanoparticles (AgONPs) in an approach that was beneficial for the natural world. The procedure worked well, was cheap, good for the environment and could be

done at room temperature. X-ray diffraction showed that the configuration was cubic and microscopy with scanning electrons showed that the particles looked like flowers with little spheres on their surfaces. Biological experiments showed that it worked against six types of bacteria, including *E. coli* and a few types of fungi. Silver nanoparticles produced from peppermint leaf extract worked more successfully against bacteria than those made from black nightshade [26].

**In 2024, Gungure et al.**, utilized the distillation coating process to make (PES/PVP/CaCO<sub>3</sub>) membranes that were composite using Ag<sub>2</sub>O. FTIR-ATR showed that there was an Ag-O bond. SEM results showed that the nanoparticles were evenly distributed and had a superior ability to absorb water. The membranes also demonstrated the ability to eliminate bacteria [27].

**In 2025, Zahra et al.**, fabricated by optimizing AgNO<sub>3</sub> concentration, reaction time, and using *Bacillus subtilis* for biological applications. The resulting nanoparticles were uniform and crystalline, with an average size of 193.9 μm, confirmed by SEM, EDX, and XRD diffraction peaks between 26.46° and 68.19°. The HA-Ag<sub>2</sub>O nano-adsorbents effectively inhibited *E. coli*, *S. aureus*, and *Lactobacillus sap*, with *S. aureus* being most susceptible. They exhibited 84.36% antioxidant activity and degraded 82.28% of methylene blue under UV irradiation in 120 minutes. This biohybrid system combines photocatalytic activity with biocompatibility, offering multifunctional potential for environmental and biomedical applications [28].

**In 2025, Daniel and Nwankwo**, published a study on the chemical deposition of silver/silver oxide (Ag/AgO) thin films on glass substrates. Silver nitrate (AgNO<sub>3</sub>) and triethanolamine were used as the main

reactants, along with auxiliary components to facilitate the reaction and improve film properties. (XRD) confirmed the crystal structure of the films, showing distinct peaks at (111), (200), (220), and (311). (SEM) verified the surface morphology, while EDS analysis confirmed the presence of all reactants. Due to the presence of silver, the films exhibited low transmittance (~12%) and high absorption (~80%) across the 300–1100 nm wavelength range in UV spectroscopy. These integrated films demonstrate potential for various applications, including water purification, photocatalysis, and optical devices [29].

### **1.7. Aims of the Work**

1. Preparing Ag, AgCl, AgO nanomaterials using different methods and studying their structural, compositional and surface properties.
- 2 . Studying the cytotoxicity and safety of the prepared nanomaterials for use in water applications, and evaluating their effectiveness in removing discoloration from water pollution.
3. Biologically applying the nanomaterials to different types of bacteria and determining the concentrations at which they achieve optimal bacterial inhibition for water purification applications.
4. Manufacturing various types of polymer membranes reinforced with prepared materials and conducting tests using different techniques to ensure the operation of the filters and their inclusion in applications for removing bacterial contaminants for water purification applications.

## الخلاصة

تم في هذه الأطروحة تصنيع أغشية بوليمرية مدمجة بمواد قائمة على الفضة لتحسين إزالة الملوثات من المياه وتكون ذات خصائص مسامية ومرنة ومضادة للبكتيريا ومحفزة ضوئياً.

تم تنفيذ العمل عبر مرحلتين رئيسيتين. في المرحلة الأولى، تم تحضير جسيمات نانوية فضية باستخدام الطريقة الكيميائية وطريقة الاستئصال بالليزر في السوائل. أما المرحلة الثانية، فقد تضمنت دمج هذه الجسيمات داخل مصفوفة بوليمرية مكونة من بولي إيثر سلفون (PES) كمادة أساسية، مع إضافة بولي فينيل بيروليدون (PVP) وكربونات الكالسيوم ( $\text{CaCO}_3$ ) كعوامل مساعدة على تكوين المسام وتحسين نفاذية الأغشية.

تم تحليل الخصائص البنيوية للجسيمات النانوية المحضرة باستخدام حيود الأشعة السينية (XRD). أظهرت أنماط العينات المحضرة كيميائياً، بالترتيب A1-AgO1 (مرجع)، A2 ( $\text{AgO-AgCl}$ )، A3 ( $\text{AgO-AgCl}$ )، وA4 ( $\text{AgO}$ )، قمم حيود واضحة عند المستويات (111)، (200)، (220)، و(311)، مما يؤكد تكون بلورات ( $\text{AgO}$ ) ذات بنية مكعبة مركزية الوجوه (FCC). لوحظت قمم إضافية في بعض العينات، وخاصة A2 وA3، تشير إلى وجود كلوريد الفضة ( $\text{AgCl}$ )، مما يدل على تكون أطوار مختلطة نتيجة لظروف التحضير. أظهرت الحسابات أن متوسط حجم البلورات في العينات المحضرة كيميائياً يبلغ حوالي 33 نانومتراً. على النقيض من ذلك، أدى استخدام الاستئصال بالليزر النبضي في السوائل للعينات A5 ( $\text{Ag-AgO}$ ) وA6 ( $\text{Ag-AgO}$ )، وأصغر حجماً وأكثر تجانساً، بمتوسط حجم بلوري يبلغ حوالي 25 نانومتراً، مما يعكس تأثير طريقة التحضير على حجم البلورات وتجانسها.

أكد تحليل طيف الأشعة تحت الحمراء (FTIR) وجود روابط  $\text{Ag-O}$  في نطاق 400-600  $\text{سم}^{-1}$ ، مما يشير إلى نجاح تكوين أكسيد الفضة. وعزيت الحزمة العريضة الملحوظة عند 3400  $\text{سم}^{-1}$  إلى اهتزازات مجموعة الهيدروكسيل المرتبطة بالرطوبة الممتصة على أسطح الجسيمات النانوية. كما لوحظت حزم أخرى متعلقة بالمجموعات الوظيفية السطحية، مما يدل على استقرار كيميائي جيد للمواد المحضرة.

أظهرت أطياف الأشعة فوق البنفسجية والمرئية (UV-Vis) أن العينات الكيميائية (A1-A4) أظهرت قمم امتصاص عند أطوال موجية أقل من 300 نانومتر، مما يشير إلى تكوين  $\text{AgO}$  و $\text{AgCl}$ . أظهرت عينات الليزر (A5-A8) قمم رنين بلازمون سطحي عند 410-427 نانومتر، مما يؤكد وجود جزيئات فضة مستقرة.

وكشفت صور المجهر الإلكتروني الماسح (SEM) عن اختلافات واضحة في الشكل والحجم تبعاً لطريقة التحضير. تألفت العينة A1 من جسيمات نانوية يتراوح حجمها بين 24 و51 نانومتر مع كتل طفيف، بينما أظهرت العينات الأخرى المحضرة كيميائياً (A2-A4) جسيمات أكبر حجماً وأكثر تبايناً يتراوح حجمها بين 205 و323 نانومتر. أما العينات المحضرة بالليزر (A5-A8) فقد أظهرت توزيعاً أكثر تجانساً للجسيمات الكروية والمكعبة، بأحجام تتراوح بين 57 و107 نانومتر، مما يدل على قدرة تقنيات الليزر على إنتاج جسيمات نانوية عالية التجانس.

وأكد تحليل طيف الأشعة السينية المشتتة للطاقة (EDS) وجود الفضة والأكسجين كمكونين رئيسيين في جميع العينات، مما يدعم نتائج حيود الأشعة السينية (XRD) وتحليل طيف الأشعة تحت الحمراء بتحويل فورييه (FTIR) فيما يتعلق بتكوين أكسيد الفضة. وكان محتوى الفضة أعلى من محتوى الأكسجين، مما يشير إلى نقاء المواد. بالإضافة إلى ذلك، أشارت قياسات جهد زينا إلى استقرار عالٍ في الوسط السائل، حيث تراوحت القيم بين 35.71 و-45.91 ملي فولت، مما يعكس وجود تنافر كهروستاتيكي كافٍ لمنع التكتل والحفاظ على التجانس، مع اختلاف أحجام الجسيمات تبعاً لطريقة التحضير.

أما من الناحية التطبيقية، فقد أظهرت الجسيمات النانوية نشاطاً بيولوجياً ملحوظاً. ازداد التأثير المضاد للبكتيريا مع زيادة التركيز ضد سلالتين من البكتيريا، مما أظهر تثبيطاً واضحاً عند التركيزات العالية.

أظهرت اختبارات السمية الخلوية للعينات A1 وA4 وA5 وA8 سمية متوسطة، حيث سجلت العينة A4 أعلى قيمة سمية بلغت 15.6.

أما من الناحية التحفيزية الضوئية، فقد أظهرت العينات كفاءة تحفيزية ضوئية جيدة في تحلل الصبغة الزرقاء الملوثة تحت الضوء المرئي، حيث بلغت كفاءة الإزالة 70% للعينة A1 و79% للعينة A3 بعد 150 دقيقة من التعريض للإشعاع.

فيما يتعلق بالأغشية البوليمرية PES/PVP المطعمة بجزيئات الفضة النانوية، أكد تحليل ATR-FTIR نجاح دمج الجزيئات النانوية ضمن المصفوفة البوليمرية. وقد أدى تطعيم أكسيد الفضة في الأغشية إلى تحسين خصائص سطحها.

انخفضت زاوية التلامس من 83° إلى 65° و58° مع زيادة محتوى أكسيد الفضة، مما يشير إلى تحسن استرطابية الأغشية. كما ارتفع معدل تدفق الماء من 82 لتر/م<sup>2</sup>/ساعة للأغشية غير المعدلة إلى 115 و132 لتر/م<sup>2</sup>/ساعة، مما يعكس زيادة نفاذية الماء.

وأظهر تحليل SEM أن الأغشية المحضرة تمتلك بنية مسامية إسفنجية ذات تجاويف وقنوات مترابطة، مما يتيح نفاذية فعالة للماء. ولوحظت في تقنية FESEM في الفحص الجانبي ان المسامات واضحة اختلافات في حجم المسام وسمك الطبقة تبعاً لطريقة التصنيع. تجدر الإشارة إلى أن الأغشية المدعمة بجزيئات نانوية مصنعة بالليزر أظهرت أداءً فائقاً في مكافحة البكتيريا، حيث بلغت معدلات التنشيط 95-99%، مما يبرز إمكانية تطبيقها الواعدة في تنقية المياه وإزالة الملوثات. وقد أكدت التقييمات البيولوجية تحسناً ملحوظاً في النشاط المضاد للبكتيريا، إذ ارتفع من 13-41% في الأغشية الأصلية إلى 72-73% عند إضافة مسحوق الفضة، ووصل إلى 95-99% بعد دمج جزيئات أكسيد الفضة النانوية المصنعة بالليزر. وبشكل عام، تظهر هذه النتائج أن تعديل أكسيد الفضة يحسن بشكل كبير من وظائف الأغشية، مما يجعلها مناسبة لتطبيقات معالجة المياه.



جمهورية العراق  
وزارة التعليم العالي  
والبحث العلمي  
جامعة ديالى  
كلية العلوم  
قسم الفيزياء

## تصنيع وتوصيف أغشية خليط PES/PVP المضمنة بمواد اساسها الفضة لتطبيقات تنقية المياه

اطروحة مقدمة الى

مجلس كلية العلوم- جامعة ديالى

جزء من متطلبات دكتوراه الفلسفة في علوم الفيزياء

من قبل

صباح علي خضر

بإشراف

أ.م.د. عمار عايش حبيب

أ.م.د. مهند مهدي عبد